

Decoding the phase structure of QCD via particle production at high energy

Anton Andronic

*Research Division and EMMI, GSI Helmholtzzentrum für Schwerionenforschung, 64291 Darmstadt, Germany and
Institut für Kernphysik, Universität Münster, 48149 Münster, Germany*

Peter Braun-Munzinger

*Research Division and EMMI, GSI Helmholtzzentrum für Schwerionenforschung, 64291 Darmstadt, Germany
Physikalisches Institut, Universität Heidelberg, 69120 Heidelberg, Germany and
Institute of Particle Physics and Key Laboratory of Quark and Lepton Physics (MOE),
Central China Normal University, Wuhan 430079, China*

Krzysztof Redlich

*University of Wrocław, Institute of Theoretical Physics, 50-204 Wrocław, Poland and
Research Division and EMMI, GSI Helmholtzzentrum für Schwerionenforschung, 64291 Darmstadt, Germany*

Johanna Stachel

Physikalisches Institut, University of Heidelberg, 69120 Heidelberg, Germany

Abstract

Recent studies based on non-perturbative lattice Monte-Carlo solutions of Quantum Chromodynamics, the theory of strong interactions, demonstrated that at high temperature there is a phase change from confined hadronic matter to a deconfined quark-gluon plasma where quarks and gluons can travel distances largely exceeding the size of hadrons. The phase structure of such strongly interacting matter can be decoded via analysis of particle abundances in high energy nuclear collisions within the framework of the statistical hadronization approach. The results imply quark-hadron duality at and experimental delineation of the location of the phase boundary of strongly interacting matter.

Atomic nuclei are bound by the strong force between their constituents, protons and neutrons, or 'nucleons'. Although the density in the center of a heavy nucleus is extremely large (about 10^{14} times the density of water), the mean distance between nucleons exceeds their diameter (the radius of the nucleon is about $0.88 \text{ fm} = 0.88 \cdot 10^{-15} \text{ m}$, and the number density inside a nucleus is $n_0 = 0.16/\text{fm}^3$). Thus in terms of the filling fraction, normal nuclear matter is dilute. If one compresses or heats such matter in high energy nuclear collisions (see, e.g., [1–3]) to even higher densities and/or high temperatures (typically of order of $k_B T \approx m_\pi c^2$ where m_π is the mass of the lightest hadron, the pion, and k_B and c are Boltzmann's constant and the speed of light), one expects [4–7] that quarks, the building blocks of nucleons, are no longer confined but can move over distances much larger than the size of the nucleon. Such a 'deconfined' state of matter, named the Quark-Gluon Plasma (QGP) [8], is likely to have existed in the Early Universe within the first microseconds after its creation in the Big Bang [9]. One of the challenging questions in modern nuclear physics is to identify the structure and phases of such strongly interacting matter [10].

Evidence for the existence, in the laboratory, of the QGP was obtained by studying collisions between heavy atomic nuclei (Au, Pb) at ultra-relativistic energies. First relevant results came from experiments at the

CERN Super-Proton-Synchrotron (SPS) accelerator [11]. With the start of operation of the Relativistic Heavy Ion Collider (RHIC) at Brookhaven National Laboratory (BNL), experiments confirmed the existence of this new state of matter and found new observables providing further strong evidence for QGP formation and expansion dynamics in the hot fireball produced in high-energy nuclear collisions. Interesting and supporting evidence was also obtained from experiments at the BNL Alternating Gradient Synchrotron (AGS) through the discovery of collective dynamics at high energy [12]. For nuclear collisions the center-of-mass energies per nucleon pair, $\sqrt{s_{NN}}$, covered by different accelerator facilities are:

1. BNL AGS, $\sqrt{s_{NN}} = 2.7 - 4.8 \text{ GeV}$
2. CERN SPS, $\sqrt{s_{NN}} = 6.2 - 17.3 \text{ GeV}$
3. BNL RHIC, $\sqrt{s_{NN}} = 7.0 - 200 \text{ GeV}$
4. CERN LHC, $\sqrt{s_{NN}} = 2.76 - 5.02 \text{ TeV}$

Importantly, the results from RHIC showed that the QGP behaves more like a nearly ideal, strongly interacting fluid rather than a weakly interacting gas of quarks and gluons [1, 3, 13–16]. These results were confirmed and extended into hitherto unexplored regions of phase space (in particular high transverse momenta) by experiments at the CERN Large Hadron Collider (LHC) [17–19]. At LHC energies the fireball formed in Pb-Pb

collisions is so hot and dense that quarks or gluons (partons) produced initially with energies of up to a few hundred GeV lose a significant fraction of their energy while traversing it.

The characterization of the QGP in terms of its equation of state (EoS) expressing pressure as function of energy density, and of its transport properties such as, e.g., its viscosity or diffusion coefficients, as well as delineating the phases of strongly interacting matter [20] is a major ongoing research effort [2, 3, 18, 21, 22]. However, it turned out that direct connections between the underlying theory of strong interactions in the standard model of particle physics, Quantum Chromodynamics (QCD) [23] and the experimental data are not readily established. This is since the constituents of the QGP, the colored quarks and gluons, are not observable as free particles, a fundamental property of QCD called 'confinement'. What is observable are colorless bound states of these partons, resulting in mesons and baryons, generally referred to as hadrons. Furthermore, the equations of QCD can only be solved analytically in the high energy and short distance limit where perturbative techniques can be used due to the asymptotic freedom property of QCD [24, 25]. This is unfortunately not possible for the QGP where typical distance scales exceed the size of the largest atomic nuclei and the typical momentum scale is low. The only presently known technique is to solve the QCD equations numerically by discretization of the QCD Lagrangian on a four-dimensional space-time lattice, and statistical evaluation via Monte Carlo methods, Lattice QCD (LQCD) [26].

Below we will discuss how the phase structure of strongly interacting matter described by LQCD can be decoded via analysis of particle production in high energy nuclear collisions. This is achieved by making use of the observed thermalization pattern of particle abundances within the framework of the statistical hadronization approach at various collision energies.

CONNECTING HADRONIC STATES AND QCD CONSTITUENTS

From LQCD calculations, a deconfinement transition from matter composed of hadronic constituents, hadronic matter, to a QGP was indeed predicted (see Ref. [26] for an early review) at an energy density of about 1 GeV/fm³. Besides deconfinement, there is also a chiral symmetry restoration transition expected in high energy density matter [27, 28].

Due to the very small masses of the up and down quarks, the equations of QCD exhibit symmetries, called chiral symmetries, that allow separate transformations among the right-handed quarks (with spin oriented in direction of momentum) and left-handed quarks. Such symmetries, however, are not manifest in the observed strongly interacting particles, as they do not come in opposite parity pairs. Thus, chiral symmetry must be spon-

taneously broken at finite energy density. Consequently, QCD predicts the existence of a chiral transition between a phase where chiral symmetry is broken, at low temperature and/or density, and a chirally-symmetric phase at high temperature and/or density. The connection between deconfinement and chiral transition is theoretically not fully understood.

It was demonstrated [29], again using the methods of LQCD, that at zero baryo-chemical potential μ_B the deconfinement transition is linked to the restoration of chiral symmetry and that it is of crossover type with a continuous, smooth but rapid increase of thermodynamic quantities in a narrow region around the pseudo-critical temperature T_c . Using here and below units such that $\hbar = 1$, $k_B = 1$, and $c = 1$, the value of T_c at vanishing μ_B is currently calculated in LQCD to be 154 ± 9 MeV [30] and 156 ± 9 MeV [31, 32] using different fermion actions, resulting in excellent agreement. Recent LQCD results also quantify the small decrease of T_c with increasing μ_B as long as $\mu_B < 3T_c$. Within this parameter range the transition is still of crossover type. A fundamental question is the possible existence of a critical end point, where a genuine second order chiral phase transition is expected. This is currently addressed both experimentally (see a review in Ref. [33]) and theoretically (see a review in Ref. [34]) and is one of the outstanding problems remaining to understand the phase structure of hot and dense QCD matter.

These results do not shed light on the mechanism of the transition from deconfinement to confinement. In fact, the crossover nature of the chiral transition raises the question whether hadron production from a deconfined medium also might happen over a wide range of temperatures and how confinement can be implemented in a smooth transition without leading to free quarks. A related question is the possible survival of colorless bound states (hadrons) in a deconfined medium. The present work attempts to shed light on some of these questions by making contact with LQCD phenomenology and the by now impressive body of results on hadron production in central collisions between two heavy atomic nuclei at high energy. Central collisions are nearly head-on collisions; centrality is calculated in experiment matching measured particle multiplicity or energy to the geometry of the collision, see details in ref. [17].

Towards that end we remark that the QCD Lagrange density is formulated entirely in terms of the basic constituents of QCD, the quarks and gluons. The masses of hadrons as colorless bound-states of quarks and gluons are well calculated within LQCD, showing remarkable agreement with experiment [35]. This confirms that chiral symmetry is broken in the QCD vacuum, reflected in the mass differences between parity partners as well as the existence of anomalously light pions as approximate Goldstone bosons associated with spontaneous symmetry breaking.

One of the consequences of confinement in QCD is that physical observables require a representation in terms of

hadronic states. Indeed, as has been noted recently in the context of QCD thermodynamics (see, e.g., [36] and refs. therein) the corresponding partition function Z can be very well approximated within the framework of the hadron resonance gas, as long as the temperature stays below T_c . To make this more transparent, we first note that all thermodynamic variables like pressure P and entropy density s can be expressed in terms of derivatives of logarithms of Z . For the pressure, e.g., we obtain for a system with volume V and temperature T :

$$\frac{p}{T^4} = \frac{1}{T^3} \frac{\partial \ln Z(V, T, \mu)}{\partial V}. \quad (1)$$

The results of [37] imply that, as long as $T \lesssim T_c$,

$$\ln Z(T, V, \mu) \approx \sum_{i \in \text{mesons}} \ln \mathcal{Z}_{M_i}^M(T, V, \mu_Q, \mu_S) + \sum_{i \in \text{baryons}} \ln \mathcal{Z}_{M_i}^B(T, V, \mu_B, \mu_Q, \mu_S), \quad (2)$$

where the partition function of the hadron resonance gas model is expressed in mesonic and baryonic components, where M_i is the mass of a given hadron. The chemical potential μ reflects then the baryonic, electric charge, and strangeness components $\mu = (\mu_B, \mu_Q, \mu_S)$.

To make this connection quantitative, detailed investigations have recently been made on the contribution of mesons and baryons to the total pressure of the matter. In particular, in [36, 38] and refs. therein, the equation of state and different fluctuation observables are evaluated in the hadronic sector via the hadron resonance gas and compared to predictions from LQCD. Very good agreement is obtained for temperatures up to very close to T_c , lending further support to the hadron-parton duality described by Eq. 2.

The partition function of the hadron resonance gas in Eq. 2 is evaluated as a mixture of ideal gases of all stable hadrons and resonances. In the spirit of the S-matrix formalism [39], which provides a consistent theoretical framework to implement interactions in a dilute many-body system in equilibrium, the presence of resonances corresponds to attractive interactions among hadrons. This is generally a good approximation since for temperatures considered here ($T < 165$ MeV) the total particle density is low, $n < 0.5/\text{fm}^3$.

Sometimes, additional repulsive interactions are modelled with an 'excluded volume' prescription, see, e.g., [37] and refs. there, which is inherently a low density approach. For weak repulsion, implying excluded volume radii $r_0 < 0.3$ fm, the effect of the correction is mainly to decrease particle densities, while the important thermal parameters T and μ_B are little affected. Strong repulsion cannot be modelled that way: significantly larger r_0 values lead to, among others, unphysical (superluminal) equations of state, in contra-distinction to results from LQCD. In the following we use $r_0 = 0.3$ fm both for mesons and baryons. All results on thermal parameters

described below are unchanged from what is obtained in the non-interacting limit except for the overall particle density which is reduced by up to 25%.

Over the course of the last 20 years it has become apparent [40–45] that the yields of all hadrons produced in central collisions can be very well described by computing particle densities from the above hadronic partition function. To obtain particle yields at a particular temperature T_{CF} and μ_B one multiplies the so obtained thermal densities with the fireball volume V . In practice, T_{CF} , μ_B , and V , the parameters at 'chemical freeze-out' from which point on all hadron yields are frozen, are determined from a fit to the experimental data. Note that V is actually the volume corresponding to a slice of one unit of rapidity, centered at mid-rapidity. Experimentally, the rapidity density dN/dy of a hadron is obtained by integration of its momentum space distribution over the momentum component transverse to the beam direction. In general we take these yields at mid-rapidity, i.e. $y = 0$, where the center of mass of the colliding system is at rest.

As will be discussed below, this 'statistical hadronization approach' provides, via Eq. 1 and Eq. 2, a link between data on hadron production in ultra-relativistic nuclear collisions and the QCD partition function. This link opens an avenue to shed light on the QCD phase diagram. The possibility of such a connection was surmised early on [6, 46] and various aspects of it were discussed more recently [44, 47–53].

The full power of this link, however, becomes apparent only with the recent precision data from the LHC. Below we will discuss the accuracy which can be achieved in the description of hadron production using the parton-hadron duality concept described above. We will first focus on hadrons containing only light quarks with flavors up, down, and strange (u,d,s) and place emphasis on LHC data. Those show matter and anti-matter production in equal amounts, therefore indicating that μ_B is very close to zero. It is in this energy region where the LQCD approach can be applied essentially without approximations using present computer technology. We then explore the lower energy region ($500 \text{ GeV} > \sqrt{s_{NN}} > 15 \text{ GeV}$) and show that, for the first time, consistent information on the QCD phase diagram for $0 < \mu_B < 300$ MeV can be achieved by quantitatively comparing LQCD predictions for finite μ_B with results from statistical hadronization analysis of hadron production data. In the last section we will discuss how the statistical hadronization approach can be extended to include heavy (charm c and bottom b) quarks. We further discuss how the recent LHC data can provide information on the hadronization of these heavy quarks during the expansion and cooling of the QGP formed in such high-energy central nuclear collisions.

STATISTICAL HADRONIZATION OF LIGHT QUARKS

The description of particle production in nucleus-nucleus collisions in the framework of the statistical hadronization approach is particularly transparent at the LHC energy where the chemical freeze-out is quantified, essentially, by the temperature T_{CF} and the volume V of the produced fireball.

The parameters of the statistical hadronization approach are obtained with considerable precision by comparing to the yields of particles measured by the ALICE collaboration [54–60]. To match the measurement, the calculations include all contributions from the strong and electromagnetic decays of high-mass resonances. For π^\pm , K^\pm , and K^0 mesons, the contributions from heavy flavor hadron decays are also included. The measurement uncertainty, σ , is accounted for as the quadratic sum of statistical and systematic uncertainties, see below.

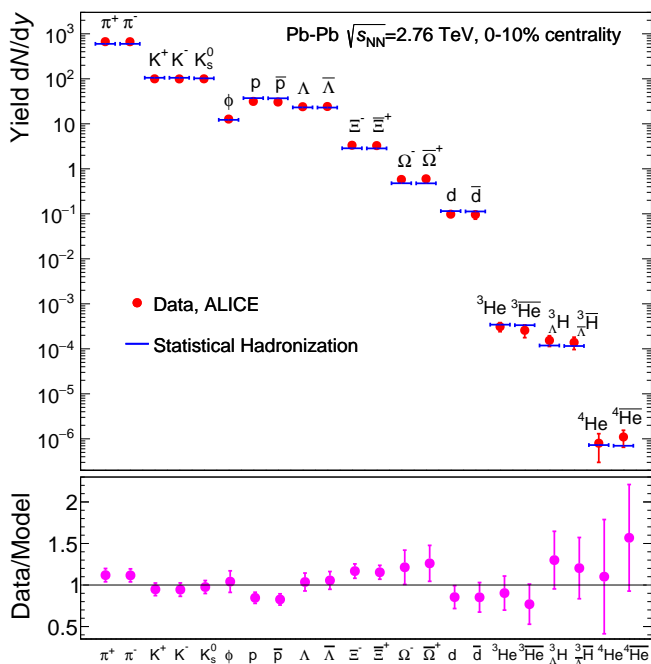


FIG. 1. Hadron abundances and statistical hadronization model predictions. Here dN/dy values for different hadrons measured at midrapidity are compared with the statistical hadronization analysis. The data are from the ALICE collaboration for central Pb–Pb collisions at the LHC. The lower panel shows the ratio of data and statistical hadronization predictions with uncertainties determined only from the data.

For the most-central Pb–Pb collisions, the best description of the ALICE data on yields of particles in one unit of rapidity at midrapidity, is obtained with $T_{CF} = 156.5 \pm 1.5$ MeV, $\mu_B = 0.7 \pm 3.8$ MeV, and $V = 5280 \pm 410$ fm³. This result is an update of the previous analysis from Ref. [45] using an extended and final set of data. The standard deviations quoted here

are exclusively due to experimental uncertainties and do not reflect the systematic uncertainties connected with the model implementation, as discussed below.

Remarkably, the value of the chemical freeze-out temperature $T_{CF} = 156.5 \pm 1.5$ MeV and the pseudo-critical temperature, $T_c = 154 \pm 9$ MeV obtained in LQCD, agree within errors. This implies that chemical freeze-out takes place close to hadronization of the QGP, lending also support to the hadron-parton duality described by Eq. 2.

A comparison of the statistical hadronization results obtained with the thermal parameters discussed above and the ALICE data for particle yields is shown in Fig. 1. Impressive overall agreement is obtained between the measured particle yields and the statistical hadronization analysis. The agreement spans nine orders of magnitude in abundance values, encompasses strange and non-strange mesons, baryons including strange and multiply-strange hyperons as well as light nuclei and hypernuclei and their anti-particles. A very small value for the baryochemical potential $\mu_B = 0.7 \pm 3.8$ MeV, consistent with zero, is obtained, as expected by the observation of equal production of matter and antimatter at the LHC [61].

The largest difference between data and calculations is observed for proton and antiproton yields, where a deviation of 2.7σ is obtained. This difference is connected with an unexpected and puzzling centrality dependence of the ratio $(p + \bar{p})/(\pi^+ + \pi^-)$ [54], see, in particular, Fig. 9 of this reference. As discussed below, the other ratios (hadrons/pions) increase towards more central collisions until a plateau (the grand-canonical limit) is reached. The peculiar behavior of the $(p + \bar{p})/(\pi^+ + \pi^-)$ at LHC energy is currently not understood. Arguments that this might be connected to annihilation of baryons in the hadronic phase after chemical freeze-out [62] are not supported by the results of recent measurements of the relative yields of strange baryons to pions [63].

A further consequence of the vanishing baryochemical potential is that also the strangeness chemical potential μ_S vanishes. This implies that the strangeness quantum number plays no role anymore for the particle production. In the fireball the yield of strange mesons and (multi-)strange baryons is exclusively determined by their mass M and spin degeneracy $(2J + 1)$ in addition to the temperature T .

The thermal origin of all particles including light nuclei and anti-nuclei is particularly transparent when inspecting the change of their yields with particle mass. This is shown in Fig. 2 where the measured yields, normalized to the spin degeneracy, are plotted as a function of the mass M . This demonstrates explicitly that the normalized yields exclusively depend on M and T . For heavy particles ($M \gg T$) without resonance decay contributions their normalized yield simply scales with mass as $M^{3/2} \exp(-M/T)$, illustrated by the nearly linear dependence observed in the logarithmic representation of Fig. 2. We note that, for the subset of light nuclei, the statistical hadronization predictions are not affected by resonance decays. For these nuclei, a small variation in

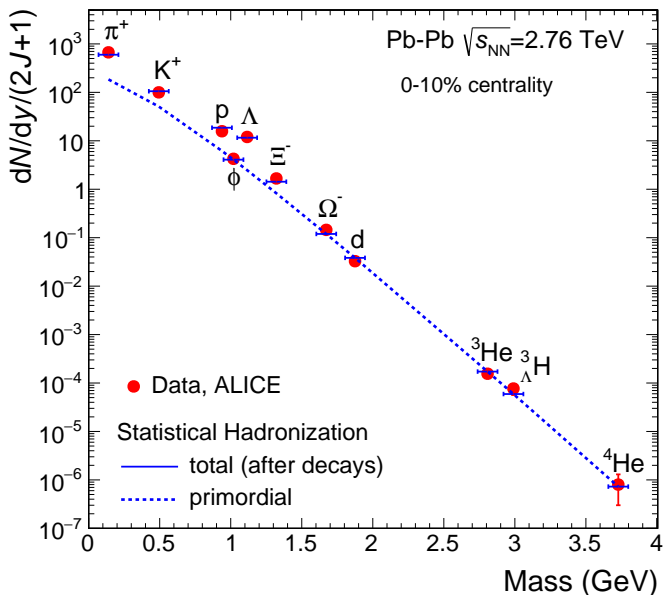


FIG. 2. Mass dependence of hadron yields compared with predictions of the statistical hadronization model. Only particles, no anti-particles, are included and the yields are divided by the spin degeneracy factor $(2J + 1)$. Data are from the ALICE collaboration for central Pb–Pb collisions at the LHC. For the statistical hadronization approach, plotted are the “total” yields, including all contributions from high-mass resonances (for the Λ hyperon, the contribution from the electromagnetic decay $\Sigma^0 \rightarrow \Lambda\gamma$, which cannot be resolved experimentally, is also included), and the (“primordial”) yields prior to strong and electromagnetic decays. For more details see text.

temperature leads to a large variation of the yield, resulting in a relatively precise determination of the freeze-out temperature $T_{nuclei} = 159 \pm 5$ MeV, well consistent with the value of T_{CF} extracted above.

The incomplete knowledge of the structure and decay probabilities of heavy mesonic and baryonic resonances discussed above leads to systematic uncertainties in the statistical hadronization approach. We note, from Fig. 2, that the yields of the measured lightest mesons and baryons, (π , K , p , Λ) are substantially increased relative to their primordial thermal production by such decay contributions. For pions, e.g., the resonance decay contribution amounts to 70%. For resonance masses larger than 1.5 GeV the individual states start to strongly overlap [23]. Consequently, neither their number density nor their decay probabilities can be determined well. Indeed, recent LQCD results indicate that there are missing resonances compared to what is listed in [23]. The resulting theoretical uncertainties are difficult to estimate but are expected to be small since T_{CF} is very small compared to their mass. A conservative estimate is that the resulting systematic uncertainty in T_{CF} is at most 3%. This is consistent with the determination of T_{CF} using only particles whose yields are not influenced by

resonance decays, see above. Until now none of these systematic uncertainties are taken into account in the statistical hadronization analysis described here.

The rapidity densities of light (anti)-nuclei and hypernuclei were actually predicted [64], based on the systematics of hadron production at lower energies. It is nevertheless remarkable that such loosely bound objects (the deuteron binding energy is 2.2 MeV, much less than $T_{nuclei} \approx 159$ or $T_{CF} \approx T_c \approx 155$ MeV) are produced with temperatures very close to that of the phase boundary at LHC energy, implying any further evolution of the fireball has to be close to isentropic. For the (anti)-hypertriton the situation is even more dramatic: this object consists of a bound state of (p , n , Λ), with a value of only 130 ± 30 keV for the energy needed to remove the Λ from it. This implies that the Λ particle is very weakly bound to a deuteron, resulting in a value for the root-mean-square size for this bound state of close to 10 fm, about the same size as that of the fireball formed in the Pb–Pb collision.

The detailed production mechanism for loosely bound states remains an open question. One, admittedly speculative, possibility is that such objects, at QGP hadronization, are produced as compact, colorless droplets of quark matter with quantum numbers of the final state hadrons. The concept of possible excitations of nuclear matter into colorless quark droplets was considered already in [65]. In our context, these states should have a lifetime of 5 fm or longer, excitation energies of 40 MeV or less, for evolution into the final state hadrons which are measured in the detector. Since by construction they are initially compact they would survive also a possible short-lived hadronic phase after hadronization. This would be a natural explanation for the striking observation of the thermal pattern for these nuclear bound states emerging from Figs. 1 and 2. Note that the observed thermal nature of their production yields is very difficult to reconcile with the assumption that these states are formed by coalescence of baryons, where the yield is proportional to a coalescence factor introduced as the square of the nuclear wave function, which actually differs strongly for the various nuclei [66, 67]. For a recent discussion of the application of coalescence models to production of loosely bound states, see [68].

One might argue that composite particles such as light nuclei and hypernuclei should not be included in the hadronic partition function described in Eq. 2. We note, however, that all nuclei, including light, loosely bound states, should result from the interaction of the fundamental QCD constituents. This is confirmed by recent LQCD calculations, see [69].

The thermal nature of particle production in ultra-relativistic nuclear collisions has been experimentally verified not only at LHC energy, but also at the lower energies of the RHIC, SPS and AGS accelerators. The essential difference is that, at these lower energies, the matter-antimatter symmetry observed at the LHC is lifted, implying non-vanishing values of the chemical po-

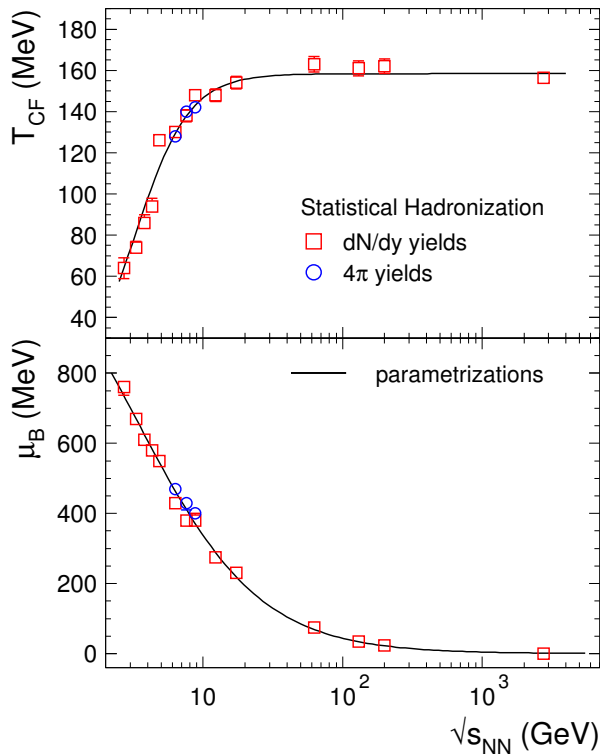


FIG. 3. Energy dependence of chemical freeze-out parameters T_{CF} and μ_B . The results are obtained from the statistical hadronization analysis of hadron yields (at midrapidity, dN/dy , and in full phase space, 4π) for central collisions at different energies. The parametrizations shown are: $T_{CF} = T_{CF}^{lim}/(1 + \exp(2.60 - \ln(\sqrt{s_{NN}})/0.45))$, $\mu_B = a/(1 + 0.288\sqrt{s_{NN}})$, with $\sqrt{s_{NN}}$ in GeV and $T_{CF}^{lim} = 158.4$ MeV and $a = 1307.5$ MeV; the uncertainty of the 'limiting temperature', T_{CF}^{lim} , determined from the fit of the 5 points for the highest energies, is 1.4 MeV.

tentials. Furthermore, in central collisions at energies below $\sqrt{s_{NN}} \approx 6$ GeV the cross section for the production of strange hadrons decreases rapidly, with the result that the average strange hadron yields per collision can be significantly below unity. In this situation, one needs to implement exact strangeness conservation in the statistical sum in Eq. 2 and apply the canonical ensemble for the conservation laws [70, 71]. Similar considerations apply for the description of particle yields in peripheral nuclear and elementary collisions. An interesting consequence of exact strangeness conservation is a suppression of strange particle yields when going from central to peripheral nucleus-nucleus collisions or from high multiplicity to low multiplicity events in proton-proton or proton-nucleus collisions. In all cases the suppression is further enhanced with increasing strangeness content of hadron. Sometimes, additional fugacity parameters g_f are introduced to account for possible non-equilibrium effects of strange and heavy flavor hadrons [44, 72]. These parameters modify the thermal yields of particles by factors

$g_f^{n_f}$, where the power n_f denotes the number of strange or heavy quarks and anti-quarks in the hadron.

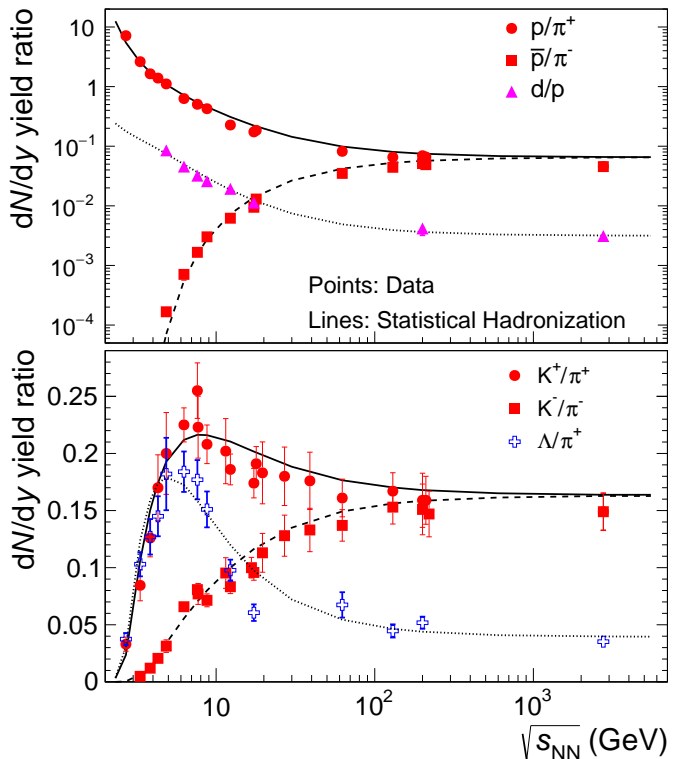


FIG. 4. Collision energy dependence of the relative abundance of several hadron species. The data (symbols) are compiled in [73, 74] and are compared to statistical hadronization calculations for the smooth parametrization of T_{CF} and μ_B as a function of energy shown in Fig. 3.

Experimental consequences of canonical thermodynamics and strangeness conservation laws have been first seen at SPS energy [75]. All above predictions are qualitatively confirmed by the striking new results from high multiplicity proton-proton and p-Pb collisions from the ALICE collaboration at LHC energy [63]. The data also explicitly exhibit the plateau in strangeness production when reaching Pb-Pb collisions which is expected when the grand-canonical region is reached, further buttressing the thermal analysis discussed above.

An intriguing observation, first made in [76], is that the overall features of hadron production in e^+e^- annihilations resemble that expected from a thermal ensemble with temperature $T \approx 160$ MeV, once exact quantum number conservation is taken into account. In these collisions, quark-antiquark pairs are produced with production yields that are not thermal but are well explained by the electro-weak standard model, see, e.g., Table II in [77]. Hadrons from these quark pairs (and sometimes gluons) appear as jets in the data. The underlying hadronisation process can be well described using statistical hadronisation model ideas [77, 78]. These studies revealed further that strangeness production deviates

significantly from a pure thermal production model and that the quantitative description of the measured yields is rather poor. Nevertheless, recognizable thermal features in e^+e^- collisions, where equilibration should be absent, may be a consequence of the generic nature of hadronization in strong interactions.

From a statistical hadronization analysis of all measured hadron yields at various beam energies the detailed energy dependence of the thermal parameters T_{CF} and μ_B has been determined [41, 51, 74, 79–82]. While μ_B decreases smoothly with increasing energy, the dependence of T_{CF} on energy exhibits a striking feature which is illustrated in Fig. 3: T_{CF} increases with increasing energy (decreasing μ_B) from about 50 MeV to about 160 MeV, where it exhibits a saturation for $\sqrt{s_{NN}} > 20$ GeV. The slight increase of this value compared to $T_{CF} = 156.5$ MeV obtained at LHC energy is due to the inclusion of points from data at RHIC energies, the details of this small difference are currently not fully understood.

The saturation of T_{CF} observed in Fig. 3 lends support to the earlier proposal [48, 50, 83] that, at least at high energies, the chemical freeze-out temperature is very close to the QCD hadronization temperature [51], implying a direct connection between data from relativistic nuclear collisions and the QCD phase boundary. This is in accord with the earlier prediction, already more than 50 years ago, by Hagedorn [84, 85] that hadronic matter cannot be heated beyond this limit. Whether there is, at the lower energies, a critical end-point [86] in the QCD phase diagram is currently at the focus of intense theoretical [19] and experimental effort [74].

To illustrate how well the thermal description of particle production in central nuclear collisions works we show, in Fig. 4, the energy dependence (excitation function) of the relative abundance of several hadron species along with the prediction using the statistical hadronization approach and the smooth evolution of the parameters (see above). Because of the interplay between the energy dependence of T_{CF} and μ_B there are characteristic features in these excitation functions. In particular, maxima appear at slightly different c.m. energies in the K^+/π^+ and Λ/π^+ ratios while corresponding anti-particle ratios exhibit a smooth behavior [87].

In the statistical approach in Eq. 2 and in the Boltzmann approximation, the density $n(\mu_B, T)$ of hadrons carrying baryon number B scales with the chemical potential as $n(\mu_B, T) \propto \exp(B\mu_B/T)$. Consequently, the ratios p/π^+ and d/p scale as $\exp(\mu_B/T)$, whereas the corresponding anti-particle ratios scale as $\exp(-\mu_B/T)$. From Fig. 3, it is apparent that μ_B/T_{CF} decreases with collision energy, accounting for the basic features of particle ratios in the upper part of Fig. 4. On the other hand, strangeness conservation unambiguously connects, for every T value, the strangeness- and baryo-chemical potentials, $\mu_S = \mu_S(\mu_B)$. As a consequence, the yields of K^+ and K^- increase and, respectively, decrease with μ_B/T . At higher energies, where T and hence pion densities saturate, the Λ/π^+ and K^+/π^+ ratios are decreasing

with energy (see lower part of Fig. 3).

We further note that, for energies beyond that of the LHC, the thermal parameter T_{CF} is determined by the QCD pseudo-critical temperature and the value of μ_B vanishes. Combined with the energy dependence of overall particle production [88] in central Pb-Pb collisions this implies that the statistical hadronization model prediction of particle yields at any energy, including those at the possible Future Circular Collider (FCC) [89] or in ultra-high energy cosmic ray collisions [90], can be made with an estimated precision of better than 15%.

Since the statistical hadronization analysis at each measured energy yields a pair of (T_{CF}, μ_B) values, these points can be used to construct a T vs. μ_B diagram, describing phenomenological constraints on the phase boundary between hadronic matter and the QGP, see Fig. 5. Note that the points at low temperature seem to converge towards the value for ground state nuclear matter ($\mu_B = 931$ MeV). As argued in [52] this limit is not necessarily connected to a phase transition. While the situation at low temperatures and collision energies is complex and at present cannot be investigated with first-principle calculations, the high temperature, high collision energy limit allows a quantitative interpretation in terms of fundamental QCD predictions.

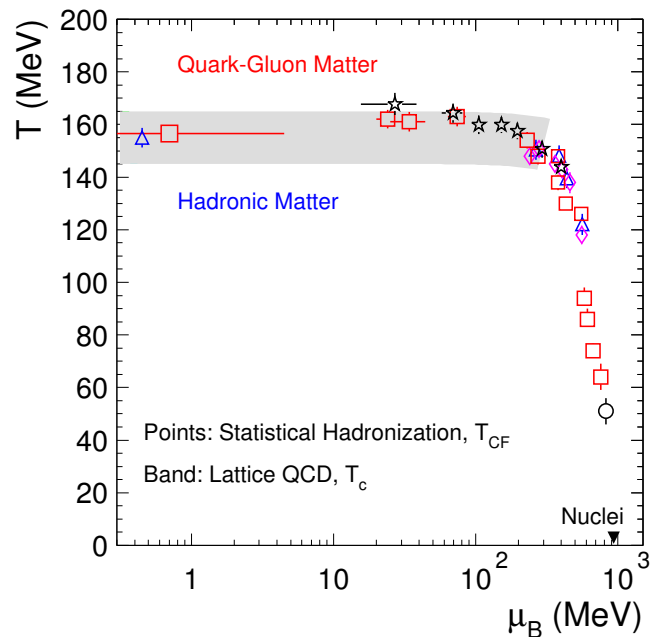


FIG. 5. Phenomenological phase diagram of strongly interacting matter constructed from chemical freeze-out points resulting from statistical hadronization analysis of hadron yields for central collisions at different energies. The freeze-out points extracted from experimental data sets in our own analysis (squares) and other similar analyses [74, 79, 91, 92] are compared to predictions from LQCD [30, 93] shown as a band. The inverted triangle marks the value for ground state nuclear matter (atomic nuclei).

The connection between LQCD predictions and experimental chemical freeze-out points is made quantitative in Fig. 5. We take here recent results for the QCD phase boundary from the two leading LQCD groups [30, 93], represented by the band in Fig. 5. As can be seen, the LQCD values follow the measured μ_B dependence of the chemical freeze-out temperature very closely, demonstrating that with relativistic nuclear collisions one can directly probe the QCD phase boundary between hadronic matter and the QGP. The above results imply that the pseudo-critical temperature of the QCD phase boundary at $\mu_B = 0$ as well as its μ_B dependence up to $\mu_B \leq 300$ MeV have been determined experimentally. There is indirect but strong evidence from measurements of the initial energy density as well as from hydrodynamical analysis of transverse momentum spectra and from the analysis of jet quenching data that initial temperatures of the fireball formed in the collision are substantially higher than the values at the phase boundary, reaching 300-600 MeV at RHIC and LHC energies [94, 95].

We close this section by remarking that the present approach can be extended beyond hadron yields to higher moments of event-by-event particle distributions. While precision predictions from LQCD exist for higher moments and susceptibilities, especially at LHC energies where μ_B is close to zero, see, e.g. [36, 38], there are formidable challenges to experimentally determine such higher moments with accuracy. Pioneering experiments were performed at the RHIC accelerator with intriguing but not yet fully conclusive results, for a recent review see [33]. Analyses of higher moments are, therefore, not considered in the present paper. Recently, however, variances of strangeness and net-baryon number fluctuations were reconstructed [96] from hadron yields measured in Pb-Pb collisions at mid-rapidity by the CERN ALICE collaboration. The so determined second moments are in impressive agreement with LQCD predictions obtained at the chiral crossover pseudo-critical temperature $T_c \approx 154$ MeV. Furthermore, an interesting strategy was proposed to compare directly experimental data on moments of net-charge fluctuations with LQCD results to identify freeze-out parameters in heavy ion collisions [97]. Within still large systematic uncertainties the extracted freeze-out parameters based on 2nd order cumulants are well consistent with statistical hadronization [98, 99]. While no formal proof of the above discussed quark-hadron duality near the chiral crossover temperature exists, the empirical evidence has recently clearly been strengthened.

STATISTICAL HADRONIZATION OF HEAVY QUARKS

An interesting question is whether the production of hadrons with heavy quarks can be described with similar statistical hadronization concepts as developed and used

in the previous section for light quarks. We note first that the masses of charm and beauty quarks, $m_c = 1.28$ GeV and $m_b = 4.18$ GeV are much larger than the characteristic scale of QCD, $\Lambda_{QCD} = 332$ MeV for three quark flavors, in the $\overline{\text{MS}}$ scheme [23]. Both masses are also sufficiently larger than the pseudo-critical temperature T_c introduced above, such that thermal production of charm and, in particular, beauty quarks is strongly Boltzmann suppressed. This is also borne out by quantitative calculations [100–102]. On the other hand we expect, in particular at LHC energies, copious production of heavy quarks in relativistic nuclear collisions through hard scattering processes which, in view of the large quark masses, can be well described using QCD perturbation theory [103]. Consequently, the charm and beauty content of the fireball formed in the nucleus-nucleus collision is determined by initial hard scattering. Furthermore, annihilation of c- and b-quarks is very small implying that their numbers are closely preserved during the fireball evolution [104].

The produced charm quarks will, therefore, not resemble a chemical equilibrium population for the temperature T . However, what is needed for the thermal description proposed below is that the heavy quarks produced in the collision reach a sufficient degree of thermal equilibrium through scattering with the partons of the hot medium. Indeed, the energy loss suffered by energetic heavy quarks in the QGP is indicative of their “strong coupling” with the medium, dominated by light quarks and gluons. The measurements at the LHC [105, 106] and RHIC [107] of the energy loss and hydrodynamic flow of D mesons demonstrate this quantitatively.

Among the various suggested probes of deconfinement, charmonium (the bound states of $c\bar{c}$) plays a distinctive role. The J/ψ meson is the first hadron for which a clear mechanism of suppression (melting) in the QGP was proposed early on, based on the color analogue of Debye screening [108]. This concept for charmonium suppression was tested experimentally at the SPS accelerator but led, with the turn-on of the RHIC facility, to a number of puzzling results. In particular, the observed rapidity and energy dependence of the suppression ran counter to the theoretical predictions [109].

However, still before publication of the first RHIC data, a novel quarkonium production mechanism, based on statistical hadronization, was proposed [72] which contained a natural explanation for the later observations at RHIC and LHC energy. The basic concept underlying this statistical hadronization approach [72] is that charm quarks are produced in initial hard collisions, subsequently thermalize in the QGP and are “distributed” into hadrons at the phase boundary, i.e. at chemical freeze-out, with thermal weights as discussed above for the light quarks, [72, 104, 110, 111]. An alternative mechanism for the (re)combination of charm and anti-charm quarks into charmonium in a QGP [112] was proposed based on kinetic theory. For further developments see [113–116].

In the statistical hadronization approach, the absence of chemical equilibrium for heavy quarks is accounted for by introducing a fugacity g_c . The parameter g_c is obtained from the balance equation [72] which accounts for the distribution of all initially produced heavy quarks into hadrons at the phase boundary, with a thermal weight constrained by exact charm conservation. With the above approach the knowledge of the heavy quark production cross section along with the thermal parameters obtained from the analysis of the yields of hadrons composed of light quarks, see previous section, is sufficient to determine the yield of hadrons containing heavy quarks in ultra-relativistic nuclear collisions.

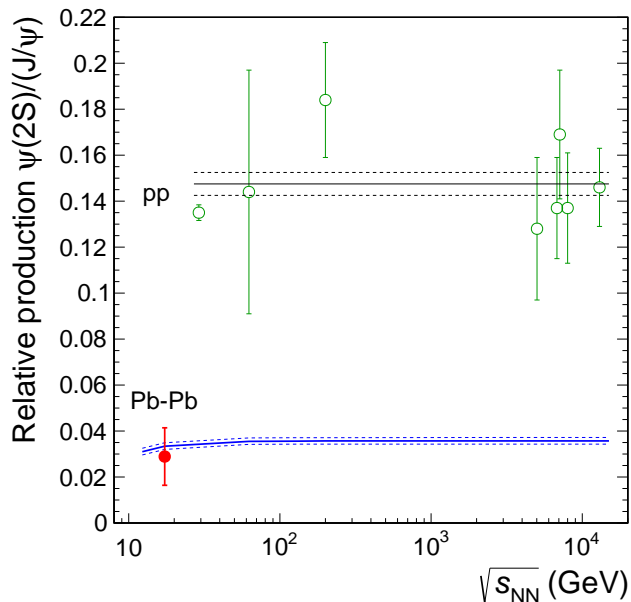


FIG. 6. Relative production of $\psi(2S)$ and J/ψ mesons as a function of collision energy. The data points for proton-proton collisions are from experiments at SPS, HERA, RHIC, and the LHC [117–122]. The point for central Pb–Pb collisions at SPS energy is from the NA50 experiment [123]. The average value of the pp measurements is represented by the black horizontal line with dashed uncertainties. The blue band denotes statistical model calculations for the temperature parameterization from heavy-ion fits, see Fig. 3.

As a consequence, a very transparent observable to verify the thermal origin of heavy flavor hadrons produced in a nuclear collision is the abundance ratio of different resonance states such as $\psi(2S)/(J/\psi)$ in the charm- or $Y(2S)/Y(1S)$ in the bottom-sector. Indeed, the first measurement of the $\psi(2S)/(J/\psi)$ abundance ratio at SPS energy [123] demonstrated that there are clearly different production mechanisms for charmonia in elementary and nuclear collisions. This is demonstrated in Fig. 6. While in elementary collisions this ratio is of the order of 0.15 and hardly varies with energy, the value observed in central Pb–Pb collisions is more than a factor of four smaller, and is remarkably consistent with the assumption that these charmonia are produced at

the phase boundary as are all other hadrons.

The chemical freeze-out temperature barely varies with energy beyond $\sqrt{s_{NN}} = 10$ GeV. Since the charm production cross section drops out in the $\psi(2S)/(J/\psi)$ ratio, the prediction of the statistical hadronization model for central Pb–Pb collisions at LHC energy is $\psi(2S)/(J/\psi) = 0.035$ with a precision indicated in Fig. 6. Recently, the ALICE collaboration released the first (p_T -integrated) data on the above ratio; the preliminary result is, within the still considerable experimental uncertainties, well consistent with the statistical hadronization prediction, lending further support for thermalization of charm quarks in the hot fireball and the production of charmed hadrons at the phase boundary.

It is also important to assess to which degree the produced charmonia participate in the hydrodynamic expansion of the fireball. This can be done by measuring the second Fourier coefficient of the angular distribution of J/ψ mesons projected onto a plane perpendicular to the beam direction, the so-called elliptic flow. Already the first measurement of J/ψ elliptic flow at the LHC [124] pointed towards rather large values of the elliptic flow coefficients. The recent measurement at $\sqrt{s_{NN}} = 5.02$ TeV from the ALICE collaboration [125] establishes the detailed flow pattern as a function of transverse momentum. The large elliptic flow observed for J/ψ mesons is similar to that observed for open charm mesons [126] and surprisingly close to the flow coefficients for light hadrons. This provides strong support for charm quark kinetic thermalization, in agreement with the statistical hadronization assumption, and implies that charm quarks couple to the medium in a similar way as light flavor quarks. Within the current statistical accuracy the J/ψ data at RHIC are compatible with a null flow signal [127]. An elliptic anisotropy signal was measured for J/ψ mesons at SPS energy [128] and was interpreted as a path-length dependence of the screening.

The response of charmonia produced in ultra-relativistic nuclear collisions to the medium of the fireball is characterized by the nuclear modification factor R_{AA} . This factor is constructed as the ratio between the rapidity densities for J/ψ mesons produced in nucleus-nucleus (AA) collisions and proton-proton collisions, scaled by the number of nucleon-nucleon collisions in a given centrality bin. Clearly, if all charmonia in the final state would originate from hard scattering processes in the initial state, $R_{AA} = 1$.

In the original color screening model [108] R_{AA} was expected to be significantly reduced from unity, and to decrease with collision centrality and energy, due to increasing energy density of the medium. The early experimental situation until 2009, i.e. before LHC turn-on, is summarized in [129]. Indeed, the first data from central Pb–Pb collisions at SPS energy showed a significant suppression which could be interpreted in terms of nuclear effects and the Debye screening mechanism. However, the data at RHIC energy exhibited a nearly

identical suppression and an unexpected peaking at mid-rapidity [129] which could not be reconciled with the predictions using the color screening model. Both observations on the energy and rapidity dependence of R_{AA} for J/ψ mesons were, however, consistent with their thermal origin [110, 130], albeit with the qualification of a rather poorly known charm production cross section.

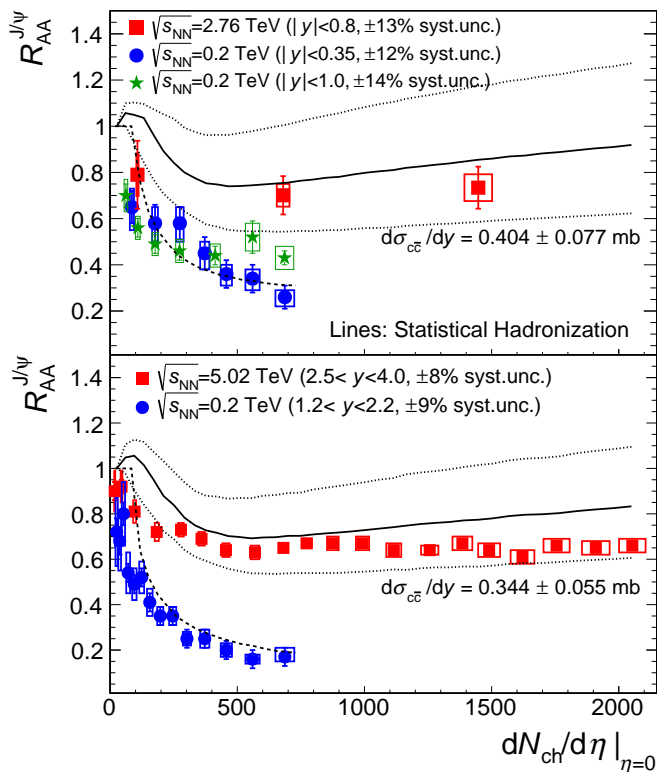


FIG. 7. The nuclear modification factor R_{AA} for inclusive J/ψ production. The dependence of R_{AA} on the multiplicity density (at $\eta=0$) for midrapidity (upper panel) and at forward rapidity (lower panel). The data are for Au–Au collisions from the PHENIX collaboration (blue) [131, 132] and STAR collaboration (green) [133] at RHIC and for Pb–Pb collisions from the ALICE collaboration (red) [134, 135] at the LHC.

In the statistical hadronization scenario, the J/ψ nuclear modification factor R_{AA} (see above) is obtained by computing the yields in AA collisions while the yields in proton-proton collisions are taken from experimental data. The so determined R_{AA} should increase with increasing collision energy, implying reduced suppression or even enhancement due to the rapid increase with energy of the charm production cross section. Clear evidence for such a pattern was obtained with the first ALICE measurements at LHC energy [134]. Since then a large number of additional data including detailed energy, rapidity, centrality and transverse momentum dependences of R_{AA} for J/ψ as well as hydrodynamic flow and $\psi(2S)/(J/\psi)$ ratio results have provided a firm basis for the statistical hadronization scenario [104], with the biggest uncertainties still related to the not yet mea-

sured value of the open charm cross section in central Pb–Pb collisions. Current results on J/ψ yields and interpretation within the statistical hadronization picture are summarized in Fig. 7. A dramatic increase of R_{AA} with increasing collision energy is clearly observed. Furthermore, newer measurements demonstrate, see e.g. Fig. 16 in [135], that the increase is largely concentrated at J/ψ transverse momentum values less than the mass $m_{J/\psi} = 3.1$ GeV. This latter observation was first predicted in Refs. [136]. Both provide further support of the original predictions from the statistical hadronization approach.

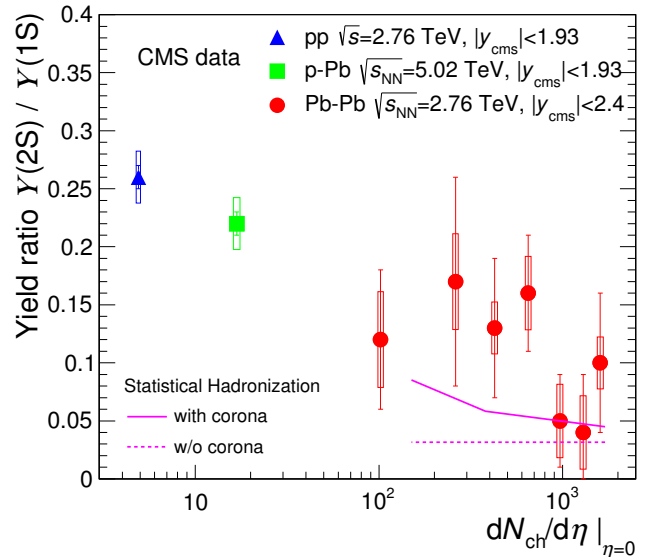


FIG. 8. Multiplicity dependence of production ratio of bottomonium states $\Upsilon(2S)$ and $\Upsilon(1S)$. The data are measured at the LHC in pp, p–Pb and Pb–Pb collisions [137]. The lines are statistical hadronization predictions for Pb–Pb collisions; the full line includes an estimate of the contribution of the production in the corona [104] of the colliding nuclei.

Recent measurements of production of bottomonium ($b\bar{b}$) states at the LHC [137–139] and at RHIC [140] can provide further insight into the understanding of the production dynamics of quarkonia in nuclear collisions. The nuclear modification factor for the Υ states exhibits at LHC energies a suppression pattern [138] not unlike that expected in the original Debye screening scenario [115]. On the other hand the observed production ratio $\Upsilon(2S)/\Upsilon(1S)$, shown in Fig. 8, also is consistent with a thermalization pattern as one approaches central collisions. Indeed, for central Pb–Pb collisions, this ratio is compatible, with the value predicted by the statistical hadronization model for $T \simeq 156$ MeV. This provides the tantalizing possibility of adding the bottom flavor as an experimental observable to constrain even further the QCD phase boundary with nucleus-nucleus collision data at high energies.

An essential ingredient of the statistical hadronization scenario for heavy quarks is that they can travel, in the

QGP, significant distances to combine with other uncorrelated partons. The observed increase of the R_{AA} for J/ψ with increasing collision energy strongly supports the notion that the mobility of the heavy quarks is such that it allows travel distances exceeding that of the typical 1 fm hadronic confinement scale. In fact, for LHC energy, the volume of a slice of one unit of rapidity of the fireball exceeds 5000 fm^3 , as shown in the previous section, implying that charm quarks can travel distances of the order of 10 fm. This results in the possibility of bound state formation with all other appropriate partons in the medium with statistical weights quantified by the characteristics of the hadron (mass, quantum numbers) at the phase boundary. The results of the charmonium measurements thereby imply a direct connection to the deconfinement properties of the strongly interacting medium created in ultra-relativistic nuclear collisions.

OUTLOOK

The phenomenological observation of the thermal nature of particle production in heavy ion collisions at the QCD phase boundary in accord with lattice QCD raises a number of challenging theoretical and experimental issues. An intriguing question is how an isolated quantum

system such as a fireball formed in relativistic nuclear collisions can reach an apparently equilibrated state. Similar questions appear [141, 142] in studies of ultra-cold quantum gases or black holes and may point to a common solution. A second area of interest is the mechanism for the formation of loosely bound nuclear states in a hot fireball at a temperature exceeding their binding energies by orders of magnitude. The question of whether there exist colorless bound states inside a deconfined QGP is related to experimentally challenging measurements of excited state populations of quarkonia.

Another priority for the field is the direct observation of the restoration of chiral symmetry and the related critical behavior in relativistic nuclear collisions with precision measurements and analysis of fluctuation observables. A highlight would be the observation of a critical endpoint in the QCD phase diagram.

Making progress with these fundamental issues is at the heart of many ongoing and future theoretical and experimental investigations.

Acknowledgements K.R. acknowledges partial support by the Extreme Matter Institute EMMI and the Polish National Science Center NCN under Maestro grant DEC-2013/10/A/ST2/00106. This work is part of and supported by the DFG Collaborative Research Center "SFB1225/ISOQUANT".

-
- [1] M. Gyulassy and L. McLerran, "New forms of QCD matter discovered at RHIC," *Nucl. Phys.* **A750** (2005) 30–63, [arXiv:nucl-th/0405013 \[nucl-th\]](#).
 - [2] P. Braun-Munzinger and J. Stachel, "The quest for the quark-gluon plasma," *Nature* **448** (2007) 302–309.
 - [3] B. V. Jacak and B. Müller, "The exploration of hot nuclear matter," *Science* **337** (2012) 310–314.
 - [4] N. Itoh, "Hydrostatic Equilibrium of Hypothetical Quark Stars," *Prog. Theor. Phys.* **44** (1970) 291.
 - [5] J. C. Collins and M. Perry, "Superdense Matter: Neutrons Or Asymptotically Free Quarks?," *Phys. Rev. Lett.* **34** (1975) 1353.
 - [6] N. Cabibbo and G. Parisi, "Exponential Hadronic Spectrum and Quark Liberation," *Phys. Lett. B* **59** (1975) 67–69.
 - [7] G. Chapline and M. Nauenberg, "Asymptotic Freedom and the Baryon-Quark Phase Transition," *Phys. Rev. D* **16** (1977) 450.
 - [8] E. V. Shuryak, "Quark-gluon plasma and hadronic production of leptons, photons and psions," *Phys. Lett. B* **78** (1978) 150.
 - [9] D. Boyanovsky, H. de Vega, and D. Schwarz, "Phase transitions in the early and the present universe," *Ann. Rev. Nucl. Part. Sci.* **56** (2006) 441–500, [arXiv:hep-ph/0602002 \[hep-ph\]](#).
 - [10] K. Rajagopal and F. Wilczek, "The Condensed matter physics of QCD," in *At the frontier of particle physics. Handbook of QCD. Vol. 1-3*, M. Shifman and B. Ioffe, eds., pp. 2061–2151. 2000. [arXiv:hep-ph/0011333 \[hep-ph\]](#).
 - [11] U. W. Heinz and M. Jacob, "Evidence for a new state of matter: An Assessment of the results from the CERN lead beam program," [arXiv:nucl-th/0002042 \[nucl-th\]](#).
 - [12] **E877** Collaboration, J. Barrette *et al.*, "Observation of anisotropic event shapes and transverse flow in Au + Au collisions at AGS energy," *Phys. Rev. Lett.* **73** (1994) 2532–2535, [arXiv:hep-ex/9405003 \[hep-ex\]](#).
 - [13] **STAR** Collaboration, J. Adams *et al.*, "Experimental and theoretical challenges in the search for the quark gluon plasma: The STAR Collaboration's critical assessment of the evidence from RHIC collisions," *Nucl. Phys. A* **757** (2005) 102–183, [arXiv:nucl-ex/0501009 \[nucl-ex\]](#).
 - [14] **BRAHMS** Collaboration, I. Arsene *et al.*, "Quark gluon plasma and color glass condensate at RHIC? The Perspective from the BRAHMS experiment," *Nucl. Phys. A* **757** (2005) 1–27, [arXiv:nucl-ex/0410020 \[nucl-ex\]](#).
 - [15] **PHENIX** Collaboration, K. Adcox *et al.*, "Formation of dense partonic matter in relativistic nucleus-nucleus collisions at RHIC: Experimental evaluation by the PHENIX collaboration," *Nucl. Phys. A* **757** (2005) 184–283, [arXiv:nucl-ex/0410003 \[nucl-ex\]](#).
 - [16] **PHOBOS** Collaboration, B. Back *et al.*, "The PHOBOS perspective on discoveries at RHIC," *Nucl. Phys. A* **757** (2005) 28–101, [arXiv:nucl-ex/0410022 \[nucl-ex\]](#).
 - [17] B. Müller, J. Schukraft, and B. Wyslouch, "First results from Pb+Pb collisions at the LHC," *Ann. Rev.*

- Nucl. Part. Sci.* **62** (2012) 361–386, [arXiv:1202.3233 \[hep-ex\]](#).
- [18] J. Schukraft, “Heavy ion physics at the Large Hadron Collider: what is new? What is next?,” *Phys. Scripta T* **158** (2013) 014003, [arXiv:1311.1429 \[hep-ex\]](#).
- [19] P. Braun-Munzinger, V. Koch, T. Schäfer, and J. Stachel, “Properties of hot and dense matter from relativistic heavy ion collisions,” *Phys. Rept.* **621** (2016) 76–126, [arXiv:1510.00442 \[nucl-th\]](#).
- [20] P. Braun-Munzinger and J. Wambach, “The Phase Diagram of Strongly-Interacting Matter,” *Rev. Mod. Phys.* **81** (2009) 1031–1050, [arXiv:0801.4256 \[hep-ph\]](#).
- [21] B. Müller, “Investigation of Hot QCD Matter: Theoretical Aspects,” *Phys. Scripta T* **158** (2013) 014004, [arXiv:1309.7616 \[nucl-th\]](#).
- [22] H. Satz, “Probing the States of Matter in QCD,” *Int. J. Mod. Phys. A* **28** (2013) 1330043, [arXiv:1310.1209 \[hep-ph\]](#).
- [23] **Particle Data Group** Collaboration, C. Patrignani *et al.*, “Review of Particle Physics,” *Chin. Phys. C* **40** no. 10, (2016) 100001.
- [24] D. J. Gross and F. Wilczek, “Ultraviolet Behavior of Nonabelian Gauge Theories,” *Phys. Rev. Lett.* **30** (1973) 1343–1346.
- [25] H. D. Politzer, “Reliable Perturbative Results for Strong Interactions?,” *Phys. Rev. Lett.* **30** (1973) 1346–1349.
- [26] F. Karsch, “Lattice QCD at high temperature and density,” *Lect. Notes Phys.* **583** (2002) 209–249, [arXiv:hep-lat/0106019 \[hep-lat\]](#).
- [27] F. Wilczek, “QCD made simple,” *Phys. Today* **53N8** (2000) 22–28.
- [28] A. Bazavov *et al.*, “The chiral and deconfinement aspects of the QCD transition,” *Phys. Rev. D* **85** (2012) 054503, [arXiv:1111.1710 \[hep-lat\]](#).
- [29] Y. Aoki, G. Endrodi, Z. Fodor, S. Katz, and K. Szabo, “The order of the quantum chromodynamics transition predicted by the standard model of particle physics,” *Nature* **443** (2006) 675–678, [arXiv:hep-lat/0611014 \[hep-lat\]](#).
- [30] **HotQCD** Collaboration, A. Bazavov *et al.*, “The equation of state in (2+1)-flavor QCD,” *Phys. Rev. D* **90** (2014) 094503, [arXiv:1407.6387 \[hep-lat\]](#).
- [31] **Wuppertal-Budapest** Collaboration, S. Borsanyi *et al.*, “Is there still any T_c mystery in lattice QCD? Results with physical masses in the continuum limit III,” *JHEP* **1009** (2010) 073, [arXiv:1005.3508 \[hep-lat\]](#).
- [32] S. Borsanyi, Z. Fodor, C. Hoelbling, S. D. Katz, S. Krieg, and K. K. Szabo, “Full result for the QCD equation of state with 2+1 flavors,” *Phys. Lett. B* **730** (2014) 99–104, [arXiv:1309.5258 \[hep-lat\]](#).
- [33] X. Luo and N. Xu, “Search for the QCD Critical Point with Fluctuations of Conserved Quantities in Relativistic Heavy-Ion Collisions at RHIC : An Overview,” *Nucl. Sci. Tech.* **28** no. 8, (2017) 112, [arXiv:1701.02105 \[nucl-ex\]](#).
- [34] F. Karsch, “The last word(s) on CPOD 2013,” *PoS CPOD2013* (2013) 046, [arXiv:1307.3978 \[hep-ph\]](#).
- [35] S. Dürr *et al.*, “Ab-Initio Determination of Light Hadron Masses,” *Science* **322** (2008) 1224–1227, [arXiv:0906.3599 \[hep-lat\]](#).
- [36] A. Bazavov *et al.*, “The QCD Equation of State to $\mathcal{O}(\mu_B^6)$ from Lattice QCD,” *Phys. Rev. D* **95** no. 5, (2017) 054504, [arXiv:1701.04325 \[hep-lat\]](#).
- [37] A. Andronic, P. Braun-Munzinger, J. Stachel, and M. Winn, “Interacting hadron resonance gas meets lattice QCD,” *Phys. Lett. B* **718** (2012) 80–85, [arXiv:1201.0693 \[nucl-th\]](#).
- [38] F. Karsch, “Thermodynamics of strong interaction matter from lattice QCD and the hadron resonance gas model,” *Acta Phys. Polon. Supp.* **7** no. 1, (2014) 117–126, [arXiv:1312.7659 \[hep-lat\]](#).
- [39] R. Dashen, S.-K. Ma, and H. J. Bernstein, “S Matrix formulation of statistical mechanics,” *Phys. Rev.* **187** (1969) 345–370.
- [40] J. Cleymans and H. Satz, “Thermal hadron production in high-energy heavy ion collisions,” *Z. Phys. C* **57** (1993) 135–148, [arXiv:hep-ph/9207204 \[hep-ph\]](#).
- [41] P. Braun-Munzinger, J. Stachel, J. Wessels, and N. Xu, “Thermal equilibration and expansion in nucleus-nucleus collisions at the AGS,” *Phys. Lett. B* **344** (1995) 43–48, [arXiv:nucl-th/9410026 \[nucl-th\]](#).
- [42] P. Braun-Munzinger, K. Redlich, and J. Stachel, “Particle production in heavy ion collisions,” *In Hwa, R.C. and Wang, X.N. (eds.): Quark-Gluon Plasma 3* (2003) 491–599, [arXiv:nucl-th/0304013 \[nucl-th\]](#).
- [43] P. Braun-Munzinger, D. Magestro, K. Redlich, and J. Stachel, “Hadron production in Au - Au collisions at RHIC,” *Phys. Lett. B* **518** (2001) 41–46, [arXiv:hep-ph/0105229 \[hep-ph\]](#).
- [44] J. Letessier and J. Rafelski, “Hadron production and phase changes in relativistic heavy ion collisions,” *Eur. Phys. J. A* **35** (2008) 221–242, [arXiv:nucl-th/0504028 \[nucl-th\]](#).
- [45] J. Stachel, A. Andronic, P. Braun-Munzinger, and K. Redlich, “Confronting LHC data with the statistical hadronization model,” *J. Phys. Conf. Ser.* **509** (2014) 012019, [arXiv:1311.4662 \[nucl-th\]](#).
- [46] R. Hagedorn, “How we got to QCD matter from the hadron side by trial and error,” *Lect. Notes Phys.* **221** (1985) 53–76.
- [47] J. Cleymans and K. Redlich, “Unified description of freezeout parameters in relativistic heavy ion collisions,” *Phys. Rev. Lett.* **81** (1998) 5284–5286, [arXiv:nucl-th/9808030 \[nucl-th\]](#).
- [48] R. Stock, “The parton to hadron phase transition observed in Pb+Pb collisions at 158-GeV per nucleon,” *Phys. Lett. B* **456** (1999) 277–282, [arXiv:hep-ph/9905247 \[hep-ph\]](#).
- [49] P. Braun-Munzinger and J. Stachel, “Particle ratios, equilibration, and the QCD phase boundary,” *J. Phys. G* **28** (2002) 1971–1976, [arXiv:nucl-th/0112051 \[nucl-th\]](#).
- [50] P. Braun-Munzinger, J. Stachel, and C. Wetterich, “Chemical freezeout and the QCD phase transition temperature,” *Phys. Lett. B* **596** (2004) 61–69, [arXiv:nucl-th/0311005 \[nucl-th\]](#).
- [51] A. Andronic, P. Braun-Munzinger, and J. Stachel, “Thermal hadron production in relativistic nuclear collisions: the hadron mass spectrum, the horn, and the QCD phase transition,” *Phys. Lett. B* **673** (2009) 142–145, [arXiv:0812.1186 \[nucl-th\]](#).
- [52] S. Floerchinger and C. Wetterich, “Chemical freeze-out in heavy ion collisions at large baryon densities,” *Nucl. Phys. A* **890-891** (2012) 11–24,

- arXiv:1202.1671 [nucl-th].
- [53] A. Bazavov *et al.*, “Freeze-out Conditions in Heavy Ion Collisions from QCD Thermodynamics,” *Phys. Rev. Lett.* **109** (2012) 192302, arXiv:1208.1220 [hep-lat].
- [54] ALICE Collaboration, B. Abelev *et al.*, “Centrality dependence of π , K, p production in Pb-Pb collisions at $\sqrt{s_{NN}} = 2.76$ TeV,” *Phys. Rev. C* **88** (2013) 044910, arXiv:1303.0737 [hep-ex].
- [55] ALICE Collaboration, B. B. Abelev *et al.*, “ K_S^0 and Λ production in Pb-Pb collisions at $\sqrt{s_{NN}} = 2.76$ TeV,” *Phys. Rev. Lett.* **111** (2013) 222301, arXiv:1307.5530 [nucl-ex].
- [56] ALICE Collaboration, B. B. Abelev *et al.*, “Multi-strange baryon production at mid-rapidity in Pb-Pb collisions at $\sqrt{s_{NN}} = 2.76$ TeV,” *Phys. Lett. B* **728** (2014) 216–227, arXiv:1307.5543 [nucl-ex].
- [57] ALICE Collaboration, B. B. Abelev *et al.*, “ $K^*(892)^0$ and $\phi(1020)$ production in Pb-Pb collisions at $\sqrt{s_{NN}} = 2.76$ TeV,” *Phys. Rev. C* **91** (2015) 024609, arXiv:1404.0495 [nucl-ex].
- [58] ALICE Collaboration, J. Adam *et al.*, “ $^3_\Lambda\text{H}$ and $^3_\Lambda\bar{\text{H}}$ production in Pb-Pb collisions at $\sqrt{s_{NN}} = 2.76$ TeV,” *Phys. Lett. B* **754** (2016) 360–372, arXiv:1506.08453 [nucl-ex].
- [59] ALICE Collaboration, J. Adam *et al.*, “Production of light nuclei and anti-nuclei in pp and Pb-Pb collisions at energies available at the CERN Large Hadron Collider,” *Phys. Rev. C* **93** no. 2, (2016) 024917, arXiv:1506.08951 [nucl-ex].
- [60] ALICE Collaboration, S. Acharya *et al.*, “Production of ^4He and $^4\bar{\text{He}}$ in Pb-Pb collisions at $\sqrt{s_{NN}} = 2.76$ TeV at the LHC,” *Nucl. Phys. A* **971** (2018) 1–20, arXiv:1710.07531 [nucl-ex].
- [61] ALICE Collaboration, B. Abelev *et al.*, “Pion, Kaon, and Proton Production in Central Pb–Pb Collisions at $\sqrt{s_{NN}} = 2.76$ TeV,” *Phys. Rev. Lett.* **109** (2012) 252301, arXiv:1208.1974 [hep-ex].
- [62] F. Becattini, E. Grossi, M. Bleicher, J. Steinheimer, and R. Stock, “Centrality dependence of hadronization and chemical freeze-out conditions in heavy ion collisions at $\sqrt{s_{NN}} = 2.76$ TeV,” *Phys. Rev. C* **90** no. 5, (2014) 054907, arXiv:1405.0710 [nucl-th].
- [63] ALICE Collaboration, J. Adam *et al.*, “Enhanced production of multi-strange hadrons in high-multiplicity proton-proton collisions,” *Nature Phys.* **13** (2017) 535–539, arXiv:1606.07424 [nucl-ex].
- [64] A. Andronic, P. Braun-Munzinger, J. Stachel, and H. Stöcker, “Production of light nuclei, hypernuclei and their antiparticles in relativistic nuclear collisions,” *Phys. Lett. B* **697** (2011) 203–207, arXiv:1010.2995 [nucl-th].
- [65] G. Chapline and A. Kerman, “On the possibility of making quark matter in nuclear collisions,” *MIT-CTP-695* (1978) .
- [66] L. P. Csernai and J. I. Kapusta, “Entropy and Cluster Production in Nuclear Collisions,” *Phys. Rept.* **131** (1986) 223–318.
- [67] S. Hirenzaki, T. Suzuki, and I. Tanihata, “A general formula of the coalescence model,” *Phys. Rev. C* **48** (1993) 2403–2408.
- [68] ExHIC Collaboration, S. Cho *et al.*, “Exotic Hadrons from Heavy Ion Collisions,” *Prog. Part. Nucl. Phys.* **95** (2017) 279–322, arXiv:1702.00486 [nucl-th].
- [69] NPLQCD Collaboration, S. R. Beane *et al.*, “Light Nuclei and Hypernuclei from Quantum Chromodynamics in the Limit of SU(3) Flavor Symmetry,” *Phys. Rev. D* **87** no. 3, (2013) 034506, arXiv:1206.5219 [hep-lat].
- [70] R. Hagedorn and K. Redlich, “Statistical Thermodynamics in Relativistic Particle and Ion Physics: Canonical or Grand Canonical?,” *Z. Phys. C* **27** (1985) 541.
- [71] S. Hamieh, K. Redlich, and A. Tounsi, “Canonical description of strangeness enhancement from p-A to Pb Pb collisions,” *Phys. Lett.* **B486** (2000) 61–66, arXiv:hep-ph/0006024 [hep-ph].
- [72] P. Braun-Munzinger and J. Stachel, “(Non)thermal aspects of charmonium production and a new look at J/ψ suppression,” *Phys. Lett. B* **490** (2000) 196–202, arXiv:nucl-th/0007059 [nucl-th].
- [73] A. Andronic, “An overview of the experimental study of quark-gluon matter in high-energy nucleus-nucleus collisions,” *Int. J. Mod. Phys. A* **29** (2014) 1430047, arXiv:1407.5003 [nucl-ex].
- [74] STAR Collaboration, L. Adamczyk *et al.*, “Bulk Properties of the Medium Produced in Relativistic Heavy-Ion Collisions from the Beam Energy Scan Program,” *Phys. Rev. C* **96** no. 4, (2017) 044904, arXiv:1701.07065 [nucl-ex].
- [75] NA57 Collaboration, F. Antinori *et al.*, “Energy dependence of hyperon production in nucleus nucleus collisions at SPS,” *Phys. Lett. B* **595** (2004) 68–74, arXiv:nucl-ex/0403022 [nucl-ex].
- [76] F. Becattini, “A thermodynamical approach to hadron production in e^+e^- collisions,” *Z. Phys. C* **69** (1996) 485–492.
- [77] F. Becattini, P. Castorina, J. Manninen, and H. Satz, “The Thermal Production of Strange and Non-Strange Hadrons in e^+e^- Collisions,” *Eur. Phys. J. C* **56** (2008) 493–510, arXiv:0805.0964 [hep-ph].
- [78] A. Andronic, F. Beutler, P. Braun-Munzinger, K. Redlich, and J. Stachel, “Thermal description of hadron production in e^+e^- collisions revisited,” *Phys. Lett. B* **675** (2009) 312–318, arXiv:0804.4132 [hep-ph].
- [79] J. Cleymans, H. Oeschler, and K. Redlich, “Influence of impact parameter on thermal description of relativistic heavy ion collisions at (1-2) A-GeV,” *Phys. Rev. C* **59** (1999) 1663, arXiv:nucl-th/9809027 [nucl-th].
- [80] P. Braun-Munzinger, I. Heppe, and J. Stachel, “Chemical equilibration in Pb + Pb collisions at the SPS,” *Phys. Lett. B* **465** (1999) 15–20, arXiv:nucl-th/9903010 [nucl-th].
- [81] J. Manninen and F. Becattini, “Chemical freeze-out in ultra-relativistic heavy ion collisions at $\sqrt{s_{NN}} = 130$ and 200 GeV,” *Phys. Rev. C* **78** (2008) 054901, arXiv:0806.4100 [nucl-th].
- [82] STAR Collaboration, B. Abelev *et al.*, “Identified particle production, azimuthal anisotropy, and interferometry measurements in Au+Au collisions at $\sqrt{s_{NN}} = 9.2$ GeV,” *Phys. Rev. C* **81** (2010) 024911, arXiv:0909.4131 [nucl-ex].
- [83] P. Braun-Munzinger and J. Stachel, “Dynamics of ultrarelativistic nuclear collisions with heavy beams: An Experimental overview,” *Nucl. Phys. A* **638** (1998)

- 3–18, [arXiv:nucl-ex/9803015](#) [nucl-ex].
- [84] R. Hagedorn, “Statistical thermodynamics of strong interactions at high-energies,” *Nuovo Cim. Suppl.* **3** (1965) 147–186.
- [85] R. Hagedorn, “Miscellaneous elementary remarks about the phase transition from a hadron gas to a Quark-Gluon Plasma,” *CERN-TH.4100* (1985) .
- [86] M. A. Stephanov, K. Rajagopal, and E. V. Shuryak, “Signatures of the tricritical point in QCD,” *Phys. Rev. Lett.* **81** (1998) 4816–4819, [arXiv:hep-ph/9806219](#) [hep-ph].
- [87] P. Braun-Munzinger, J. Cleymans, H. Oeschler, and K. Redlich, “Maximum relative strangeness content in heavy ion collisions around 30 GeV/A,” *Nucl. Phys. A* **697** (2002) 902–912, [arXiv:hep-ph/0106066](#) [hep-ph].
- [88] ALICE Collaboration, J. Adam *et al.*, “Centrality dependence of the charged-particle multiplicity density at midrapidity in Pb-Pb collisions at $\sqrt{s_{NN}} = 5.02$ TeV,” *Phys. Rev. Lett.* **116** no. 22, (2016) 222302, [arXiv:1512.06104](#) [nucl-ex].
- [89] A. Dainese *et al.*, “Heavy ions at the Future Circular Collider,” *CERN Yellow Report* **3** (2017) 635, [arXiv:1605.01389](#) [hep-ph].
- [90] Pierre Auger Collaboration, K.-H. Kampert, “Ultra-High Energy Cosmic Rays: Recent Results and Future Plans of Auger,” in *Carpathian Summer School of Physics 2016: Exotic Nuclei and Nuclear/Particle Astrophysics (VI) (CSSP16) Sinaia, Romania, June 26-July 9, 2016*. 2016. [arXiv:1612.08188](#) [astro-ph.HE].
- [91] V. Vovchenko, V. V. Begun, and M. I. Gorenstein, “Hadron multiplicities and chemical freeze-out conditions in proton-proton and nucleus-nucleus collisions,” *Phys. Rev. C* **93** no. 6, (2016) 064906, [arXiv:1512.08025](#) [nucl-th].
- [92] F. Becattini, J. Steinheimer, R. Stock, and M. Bleicher, “Hadronization conditions in relativistic nuclear collisions and the QCD pseudo-critical line,” *Phys. Lett. B* **764** (2017) 241–246, [arXiv:1605.09694](#) [nucl-th].
- [93] S. Borsanyi *et al.*, “QCD equation of state at nonzero chemical potential: continuum results with physical quark masses at order μ^2 ,” *JHEP* **1208** (2012) 053, [arXiv:1204.6710](#) [hep-lat].
- [94] PHENIX Collaboration, A. Adare *et al.*, “Enhanced production of direct photons in Au+Au collisions at $\sqrt{s_{NN}} = 200$ GeV and implications for the initial temperature,” *Phys. Rev. Lett.* **104** (2010) 132301, [arXiv:0804.4168](#) [nucl-ex].
- [95] ALICE Collaboration, J. Adam *et al.*, “Direct photon production in Pb-Pb collisions at $\sqrt{s_{NN}} = 2.76$ TeV,” *Phys. Lett. B* **754** (2016) 235–248, [arXiv:1509.07324](#) [nucl-ex].
- [96] P. Braun-Munzinger, A. Kalweit, K. Redlich, and J. Stachel, “Confronting fluctuations of conserved charges in central nuclear collisions at the LHC with predictions from Lattice QCD,” *Phys. Lett. B* **747** (2015) 292–298, [arXiv:1412.8614](#) [hep-ph].
- [97] F. Karsch, “Determination of Freeze-out Conditions from Lattice QCD Calculations,” *Central Eur. J. Phys.* **10** (2012) 1234–1237, [arXiv:1202.4173](#) [hep-lat].
- [98] S. Borsanyi, Z. Fodor, S. D. Katz, S. Krieg, C. Ratti, and K. K. Szabo, “Freeze-out parameters from electric charge and baryon number fluctuations: is there consistency?,” *Phys. Rev. Lett.* **113** (2014) 052301, [arXiv:1403.4576](#) [hep-lat].
- [99] PHENIX Collaboration, A. Adare *et al.*, “Measurement of higher cumulants of net-charge multiplicity distributions in Au+Au collisions at $\sqrt{s_{NN}} = 7.7 - 200$ GeV,” *Phys. Rev. C* **93** no. 1, (2016) 011901, [arXiv:1506.07834](#) [nucl-ex].
- [100] P. Braun-Munzinger and K. Redlich, “Charmonium production from the secondary collisions at LHC energy,” *Eur. Phys. J. C* **16** (2000) 519–525, [arXiv:hep-ph/0001008](#) [hep-ph].
- [101] B.-W. Zhang, C.-M. Ko, and W. Liu, “Thermal charm production in a quark-gluon plasma in Pb-Pb collisions at $\sqrt{s_{NN}} = 5.5$ TeV,” *Phys. Rev. C* **77** (2008) 024901, [arXiv:0709.1684](#) [nucl-th].
- [102] K. Zhou, Z. Chen, C. Greiner, and P. Zhuang, “Thermal Charm and Charmonium Production in Quark Gluon Plasma,” *Phys. Lett. B* **758** (2016) 434–439, [arXiv:1602.01667](#) [hep-ph].
- [103] M. Cacciari, S. Frixione, N. Houdeau, M. L. Mangano, P. Nason, and G. Ridolfi, “Theoretical predictions for charm and bottom production at the LHC,” *JHEP* **10** (2012) 137, [arXiv:1205.6344](#) [hep-ph].
- [104] A. Andronic, P. Braun-Munzinger, K. Redlich, and J. Stachel, “Statistical hadronization of heavy quarks in ultra-relativistic nucleus-nucleus collisions,” *Nucl. Phys. A* **789** (2007) 334–356, [arXiv:nucl-th/0611023](#) [nucl-th].
- [105] ALICE Collaboration, B. Abelev *et al.*, “Suppression of high transverse momentum D mesons in central Pb-Pb collisions at $\sqrt{s_{NN}} = 2.76$ TeV,” *JHEP* **1209** (2012) 112, [arXiv:1203.2160](#) [nucl-ex].
- [106] ALICE Collaboration, B. Abelev *et al.*, “D meson elliptic flow in non-central Pb-Pb collisions at $\sqrt{s_{NN}} = 2.76$ TeV,” *Phys. Rev. Lett.* **111** (2013) 102301, [arXiv:1305.2707](#) [nucl-ex].
- [107] STAR Collaboration, L. Adamczyk *et al.*, “Observation of D^0 meson nuclear modifications in Au+Au collisions at $\sqrt{s_{NN}} = 200$ GeV,” *Phys. Rev. Lett.* **113** (2014) 142301, [arXiv:1404.6185](#) [nucl-ex].
- [108] T. Matsui and H. Satz, “ J/ψ suppression by quark-gluon plasma formation,” *Phys. Lett. B* **178** (1986) 416.
- [109] R. Vogt, “ J/ψ production and suppression,” *Phys. Rept.* **310** (1999) 197–260.
- [110] P. Braun-Munzinger and J. Stachel, “Charmonium from statistical hadronization of heavy quarks: a probe for deconfinement in the quark-gluon plasma,” *Landolt-Börnstein* **I/23** (2010) 6.53, [arXiv:0901.2500](#) [nucl-th].
- [111] A. Andronic, P. Braun-Munzinger, K. Redlich, and J. Stachel, “The thermal model on the verge of the ultimate test: particle production in Pb-Pb collisions at the LHC,” *J. Phys. G* **38** (2011) 124081, [arXiv:1106.6321](#) [nucl-th].
- [112] R. L. Thews, M. Schroedter, and J. Rafelski, “Enhanced J/ψ production in deconfined quark matter,” *Phys. Rev. C* **63** (2001) 054905, [arXiv:hep-ph/0007323](#) [hep-ph].
- [113] Y.-P. Liu, Z. Qu, N. Xu, and P.-F. Zhuang, “ J/ψ transverse momentum distribution in high energy

- nuclear collisions at RHIC,” *Phys. Lett. B* **678** (2009) 72–76, [arXiv:0901.2757 \[nucl-th\]](#).
- [114] L. Grandchamp, R. Rapp, and G. E. Brown, “In medium effects on charmonium production in heavy ion collisions,” *Phys. Rev. Lett.* **92** (2004) 212301, [arXiv:hep-ph/0306077 \[hep-ph\]](#).
- [115] A. Emerick, X. Zhao, and R. Rapp, “Bottomonia in the quark-gluon plasma and their production at RHIC and LHC,” *Eur. Phys. J. A* **48** (2012) 72, [arXiv:1111.6537 \[hep-ph\]](#).
- [116] K. Zhou, N. Xu, Z. Xu, and P. Zhuang, “Medium effects on charmonium production at ultrarelativistic energies available at the CERN Large Hadron Collider,” *Phys. Rev. C* **89** (2014) 054911, [arXiv:1401.5845 \[nucl-th\]](#).
- [117] **NA51** Collaboration, M. C. Abreu *et al.*, “ J/ψ , ψ' and Drell-Yan production in pp and pd interactions at 450 GeV/c,” *Phys. Lett. B* **438** (1998) 35–40.
- [118] **HERA-B** Collaboration, I. Abt *et al.*, “A Measurement of the ψ' to J/ψ production ratio in 920-GeV proton-nucleus interactions,” *Eur. Phys. J. C* **49** (2007) 545–558, [arXiv:hep-ex/0607046 \[hep-ex\]](#).
- [119] **PHENIX** Collaboration, A. Adare *et al.*, “Measurement of the relative yields of $\psi(2S)$ to $\psi(1S)$ mesons produced at forward and backward rapidity in $p+p$, $p+Al$, $p+Au$, and ^3He+Au collisions at $\sqrt{s_{NN}} = 200$ GeV,” *Phys. Rev. C* **95** no. 3, (2017) 034904, [arXiv:1609.06550 \[nucl-ex\]](#).
- [120] **LHCb** Collaboration, R. Aaij *et al.*, “Measurement of J/ψ production in pp collisions at $\sqrt{s} = 7$ TeV,” *Eur. Phys. J. C* **71** (2011) 1645, [arXiv:1103.0423 \[hep-ex\]](#).
- [121] **LHCb** Collaboration, R. Aaij *et al.*, “Measurement of $\psi(2S)$ meson production in pp collisions at $\sqrt{s}=7$ TeV,” *Eur. Phys. J. C* **72** (2012) 2100, [arXiv:1204.1258 \[hep-ex\]](#).
- [122] **ALICE** Collaboration, S. Acharya *et al.*, “Energy dependence of forward-rapidity J/ψ and $\psi(2S)$ production in pp collisions at the LHC,” *Eur. Phys. J. C* **77** no. 6, (2017) 392, [arXiv:1702.00557 \[hep-ex\]](#).
- [123] **NA50** Collaboration, B. Alessandro *et al.*, “ ψ' production in Pb-Pb collisions at 158 GeV/nucleon,” *Eur. Phys. J. C* **49** (2007) 559–567, [arXiv:nucl-ex/0612013 \[nucl-ex\]](#).
- [124] **ALICE** Collaboration, E. Abbas *et al.*, “ J/ψ elliptic flow in Pb–Pb Collisions at $\sqrt{s_{NN}}=2.76$ TeV,” *Phys. Rev. Lett.* **111** (2013) 162301, [arXiv:1303.5880 \[nucl-ex\]](#).
- [125] **ALICE** Collaboration, S. Acharya *et al.*, “ J/ψ elliptic flow in Pb-Pb collisions at $\sqrt{s_{NN}} = 5.02$ TeV,” *Phys. Rev. Lett.* **119** no. 24, (2017) 242301, [arXiv:1709.05260 \[nucl-ex\]](#).
- [126] **ALICE** Collaboration, S. Acharya *et al.*, “D-meson azimuthal anisotropy in mid-central Pb-Pb collisions at $\sqrt{s_{NN}} = 5.02$ TeV,” *Phys. Rev. Lett.* **120** (2018) 102301, [arXiv:1707.01005 \[nucl-ex\]](#).
- [127] **STAR** Collaboration, L. Adamczyk *et al.*, “Measurement of J/ψ azimuthal anisotropy in Au+Au collisions at $\sqrt{s_{NN}} = 200$ GeV,” *Phys. Rev. Lett.* **111** (2013) 052301, [arXiv:1212.3304 \[nucl-ex\]](#).
- [128] **NA50** Collaboration, F. Prino *et al.*, “ J/ψ azimuthal anisotropy relative to the reaction plane in Pb-Pb collisions at 158 GeV per nucleon,” *Eur. Phys. J. C* **61** (2009) 853–858, [arXiv:0906.5376 \[nucl-ex\]](#).
- [129] L. Kluberg and H. Satz, “Color deconfinement and charmonium production in nuclear collisions,” *Landolt-Börnstein* **I/23** (2010) 6.1, [arXiv:0901.3831 \[hep-ph\]](#).
- [130] A. Andronic, P. Braun-Munzinger, K. Redlich, and J. Stachel, “Evidence for charmonium generation at the phase boundary in ultra-relativistic nuclear collisions,” *Phys. Lett. B* **652** (2007) 259–261, [arXiv:nucl-th/0701079 \[NUCL-TH\]](#).
- [131] **PHENIX** Collaboration, A. Adare *et al.*, “ J/ψ production vs centrality, transverse momentum, and rapidity in Au+Au collisions at $\sqrt{s_{NN}} = 200$ GeV,” *Phys. Rev. Lett.* **98** (2007) 232301, [arXiv:nucl-ex/0611020 \[nucl-ex\]](#).
- [132] **PHENIX** Collaboration, A. Adare *et al.*, “ J/ψ suppression at forward rapidity in Au+Au collisions at $\sqrt{s_{NN}} = 200$ GeV,” *Phys. Rev. C* **84** (2011) 054912, [arXiv:1103.6269 \[nucl-ex\]](#).
- [133] **STAR** Collaboration, L. Adamczyk *et al.*, “ J/ψ production at low p_T in Au+Au and Cu+Cu collisions at $\sqrt{s_{NN}} = 200$ GeV at STAR,” *Phys. Rev. C* **90** no. 2, (2014) 024906, [arXiv:1310.3563 \[nucl-ex\]](#).
- [134] **ALICE** Collaboration, B. B. Abelev *et al.*, “Centrality, rapidity and transverse momentum dependence of J/ψ suppression in Pb-Pb collisions at $\sqrt{s_{NN}} = 2.76$ TeV,” *Phys. Lett. B* **743** (2014) 314–327, [arXiv:1311.0214 \[nucl-ex\]](#).
- [135] **ALICE** Collaboration, J. Adam *et al.*, “ J/ψ suppression at forward rapidity in Pb-Pb collisions at $\sqrt{s_{NN}} = 5.02$ TeV,” *Phys. Lett. B* **766** (2017) 212–224, [arXiv:1606.08197 \[nucl-ex\]](#).
- [136] X. Zhao and R. Rapp, “Medium modifications and production of charmonia at LHC,” *Nucl. Phys. A* **859** (2011) 114–125, [arXiv:1102.2194 \[hep-ph\]](#).
- [137] **CMS** Collaboration, S. Chatrchyan *et al.*, “Event activity dependence of $\Upsilon(nS)$ production in $\sqrt{s_{NN}}=5.02$ TeV pPb and $\sqrt{s}=2.76$ TeV pp collisions,” *JHEP* **04** (2014) 103, [arXiv:1312.6300 \[nucl-ex\]](#).
- [138] **CMS** Collaboration, S. Chatrchyan *et al.*, “Observation of sequential Υ suppression in PbPb collisions,” *Phys. Rev. Lett.* **109** (2012) 222301, [arXiv:1208.2826 \[nucl-ex\]](#).
- [139] **ALICE** Collaboration, B. B. Abelev *et al.*, “Suppression of $\Upsilon(1S)$ at forward rapidity in Pb–Pb collisions at $\sqrt{s_{NN}} = 2.76$ TeV,” *Phys. Lett. B* **738** (2014) 361–372, [arXiv:1405.4493 \[nucl-ex\]](#).
- [140] **PHENIX** Collaboration, A. Adare *et al.*, “Measurement of $\Upsilon(1S + 2S + 3S)$ production in $p + p$ and Au+Au collisions at $\sqrt{s_{NN}} = 200$ GeV,” *Phys. Rev. C* **91** no. 2, (2015) 024913, [arXiv:1404.2246 \[nucl-ex\]](#).
- [141] M. Rigol, V. Dunjko, and M. Olshanii, “Thermalization and its mechanism for generic isolated quantum systems,” *Nature* **452** (2008) 854–858.
- [142] M. Gring *et al.*, “Relaxation and prethermalization in an isolated quantum system,” *Science* **337** no. 6100, (2012) 1318–1322, [arXiv:1112.0013 \[cond-mat\]](#).